Comparative study of room- and high-temperature Si(111)-$(\sqrt{3}\times\sqrt{3})R30°$-Au structures using one-beam RHEED intensity rocking-curve analysis

Elena A. Khramtsova
Department of Quantum Engineering, Nagoya University, Furo-cho, Chikusa-ku, Nagoya 464-01, Japan and Institute of Automation and Control Processes, 5 Radio Street, Vladivostok 690041, Russia

Ayahiko Ichimiya
Department of Quantum Engineering, Nagoya University, Furo-cho, Chikusa-ku, Nagoya 464-01, Japan
(Received 6 November 1997)

The temperature dependence of the structure perpendicular to the surface of the $\sqrt{3}\times\sqrt{3}$-Au surface phase has been studied using intensity rocking-curve analysis of one-beam RHEED. It has been found that the intensity rocking curve of the surface transforms continuously as the temperature of the substrate is increased. The transition completes at about 850 K: The rocking curve remains the same up to a temperature of about 1100 K when Au desorbtion starts. Analysis of the experimental data using dynamical one-beam calculations shows that heating of the $\alpha(\sqrt{3}\times\sqrt{3})$-Au surface with domain walls leads to the formation of a new phase, which we denote $\gamma(\sqrt{3}\times\sqrt{3})$-Au. In this paper the atomic structures perpendicular to the surface for both phases are presented and a possible mechanism of the phase transition is discussed. [S0163-1829(98)04715-8]

INTRODUCTION

Since its observation in 1969,[1] the Si(111)$(\sqrt{3}\times\sqrt{3})R30°$-Au (simply $\sqrt{3}$-Au) structure has attracted considerable attention from both theoreticians and experimentalists because of its interesting atomic structure and properties. Different from most metal-induced reconstructions of the Si(111) surface, the long-range order of the $\sqrt{3}$-Au structure is always broken up with domain walls (DW's), which separate domains of commensurate phases and form a globally incommensurate structure.[2,3] The DW spacing decreases continuously (from about 100 Å) as the metal coverage is increased. However, at high temperatures (700–900 K), as reported by Nagao *et al.*,[4] the structure of the surface is different: The DW disappears and the perfect $\sqrt{3}$-Au layer covers the whole surface. In diffraction patterns of the $\sqrt{3}$-Au surface, DW's produce diffuse rings, which surround diffraction spots at room temperature[5] (RT) and vanish at high temperature (HT) when DW's disappear.[4] This transformation is reversible and occurs under the condition of fixed coverage, that is, when an incommensurate-commensurate phase transition takes place.

This study has been undertaken in order to compare the structure perpendicular to the surface of the RT and HT $\sqrt{3}$-Au phases and to understand the atomic processes that occur during the incommensurate-commensurate phase transition. For atomic structure determination, the reflection high-energy electron diffraction (RHEED) intensity rocking curves (RC's) for one-beam condition have been measured and analyzed by RHEED dynamical calculations.[6–8] We present here the atomic structure perpendicular to the surface for the RT and HT $\sqrt{3}$-Au phases and discuss the composition and type of structural defects of both surfaces.

EXPERIMENT

All experiments were carried out in an ultrahigh vacuum (UHV) system with a base pressure of 2×10^{-10} Torr equipped with a RHEED apparatus, as described previously.[9] The incident electron beam energy was 10 keV. *N*-type (P-doped), 6.5-Ω cm Si(111) single-crystal wafers were used as samples. The surface orientation was specified as $\pm1°$ off the (111) orientation. Before introduction into the UHV chamber, the substrates were cleaned in an acetone ultrasonic bath. An atomically clean silicon surface was prepared *in situ* by direct current heating to 1500 K at pressures below 4×10^{-10} Torr. After this treatment the RHEED pattern displayed the 7×7 structure without any features corresponding to the SiC species. Gold was deposited from a W boat onto the Si(111) 7×7 surface kept at 870 K. The pressure during Au evaporation was usually about $(4-6)\times10^{-10}$ Torr and never exceeded 1×10^{-9} Torr. The deposition rate was estimated to be about 0.05 ML/min [where 1 ML is defined to be 7.8×10^{14} cm^{-2}, the ideal density of the Si(111) plane]. The evolution of the surface structure during evaporation was monitored with RHEED.

ONE-BEAM DYNAMICAL CALCULATIONS

High-energy electrons are scattered dominantly in the forward direction by atoms. Therefore, dynamic diffraction mainly occurs in the forward direction. Using this feature, it is possible to choose an orientation of the incident beam at which electrons are diffracted mainly by lattice planes parallel to the surface. This diffraction condition was named the one-beam condition,[7] as the main diffraction beam is simply a specular one. For this condition a rocking curve of the specular reflection intensity is a function of surface normal components of atomic positions, but scarcely depends on their lateral components.

The wave function of fast electrons for the one-beam condition is given by

$$\psi(\mathbf{r})=\varphi(z)\exp(i\mathbf{K}_t\cdot\mathbf{r}_t), \tag{1}$$

where z and $\mathbf{r}_t$ are surface normal and parallel components of the position vector $\mathbf{r}$ and $\mathbf{K}_t$ is the surface parallel component of the wave vector. Using Eq. (1), the Schrödinger equation for the electrons becomes

$$-\frac{\hbar^2}{2m}\frac{d^2}{dz^2}\varphi(z)-eV(z)\varphi(z)=E_z\varphi(z), \tag{2}$$

where $V(z)$ is a complex mean potential including an imaginary potential at z, E_z is the surface normal component of the kinetic energy of incident electrons, and m, $\hbar$, and e are the ordinary physical constants. According to the multislice RHEED dynamical theory,[6] the transfer matrix $\mathbf{P}_j$ at the jth slice is

$$\mathbf{P}_j=\begin{pmatrix}\tau_j & \rho_j\\ \rho_j & \tau_j\end{pmatrix}\begin{pmatrix}\exp(-i\gamma_j\cdot\Delta z_j) & 0\\ 0 & \exp(-i\gamma_j\cdot\Delta z_j)\end{pmatrix}\times\begin{pmatrix}X_j & Y_j\\ Y_j & X_j\end{pmatrix}, \tag{3}$$

where

$$\tau_j=\Gamma+\gamma_j,\quad \rho_j=\Gamma-\gamma_j,$$

$$X_j=\frac{\Gamma+\gamma_j}{4\Gamma\gamma_j},\quad Y_j=\frac{\Gamma-\gamma_j}{4\Gamma\gamma_j},$$

$$\Gamma=\sqrt{(2m/\hbar^2)E_z},\quad \gamma_j=\sqrt{\Gamma^2+(2me/\hbar^2)V(z_j)},$$

and

$$\Delta z_j=z_j-z_{j-1}.$$

The RHEED intensity is obtained easily from products of the transfer matrices as described in a paper.[6]

In this study the dynamical one-beam calculation for the $[21\bar{3}]$ azimuth was conducted with the parameters for the surface interlayer distances and atomic densities of each layer. For the $[21\bar{3}]$ incidence, the RC is recognized as approximately the RC at the one-beam condition by the many-beam dynamical calculation. Figure 1 presents RC's for the $[21\bar{3}]$ azimuth of the bulklike truncated Si(111) surface. The results of the one-beam and five-beam dynamical calculations are shown by the solid and dotted lines, respectively. As one can see, the many-beam RC is very similar to one-beam RC and many-beam effects become significant at glancing angles higher than about 5°.

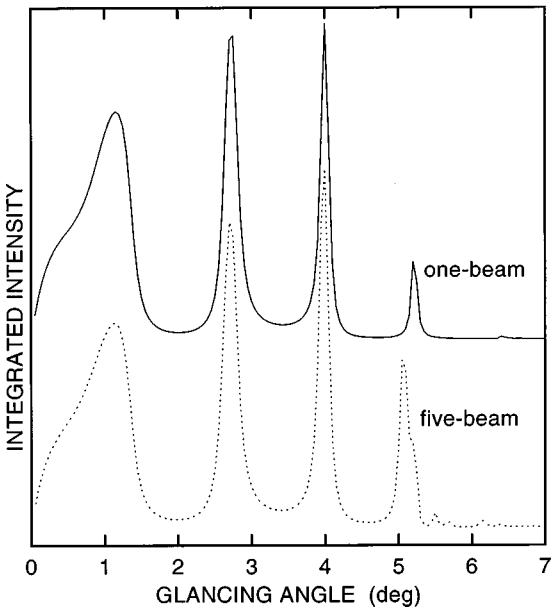

FIG. 1. Calculated RC's for the $[21\bar{3}]$ azimuth of the bulklike truncated Si(111) surface. Results of the one-beam and five-beam dynamical calculations are shown with the solid and dotted lines, respectively.

RESULTS AND DISCUSSION

Figure 2 shows the changes of the surface structure vs gold deposition time at substrate temperature (T_s) of 870 K. For the one-beam RC analysis Au deposition was stopped at 24 min; the corresponding RHEED patterns at $T_s=870$ K and RT are shown in Figs. 3(a) and 3(b), respectively.

The notation of the $\alpha\sqrt{3}$-Au is commonly accepted in the literature for the RT $\sqrt{3}$-Au structure. We shall use the $\gamma\sqrt{3}$-Au notation for the HT $\sqrt{3}$-Au surface as the $\beta\sqrt{3}$-Au one is occupied for the disordered 6×6-Au structure. Figure 4(a) shows the experimental RC's taken at $[21\bar{3}]$ incidence for the $\alpha\sqrt{3}$-Au and $\gamma\sqrt{3}$-Au structures with open and filled circles, respectively.

It should be noted that structural information-bearing features of the RC's are the positions of peaks, but not their relative intensity. The availability of electron intensity at particular angles is also very important, i.e., features such as peak shoulders or nonzero intensity plateau areas between two peaks must be taken into account. That means that the RC's presented in Fig. 4(a) are the same in the 0°–2.75° region and different at angles higher than ~2.75°. As one can see, the 2.75° and 4° peaks have shoulders and the peak at 5.30° shifts to 5.35° when T_s changes from RT to 870 K. This transformation is continuous with the temperature; the peak shoulders decrease gradually when T_s increases. In corresponding RHEED patterns, diffuse rings, which surround diffraction spots and are seen clearly in Fig. 3(b), vanish gradually and disappear completely around $T_s=850$ K, as seen in Fig. 3(a), which corresponds to the temperature when the RC transforms into the one shown in Fig. 4(a) with open circles. These experimental data are in agreement with the scanning tunnel microscope (STM) RHEED study of Nagao *et al.*,[4] who reported that at high temperatures (700–900 K)

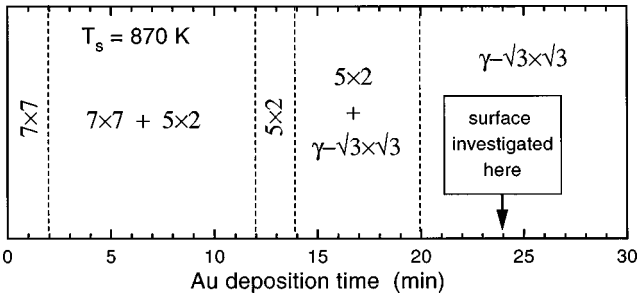

FIG. 2. Sequence of the RHEED patterns during Au deposition onto the Si(111)7×7 surface kept at 870 °C.

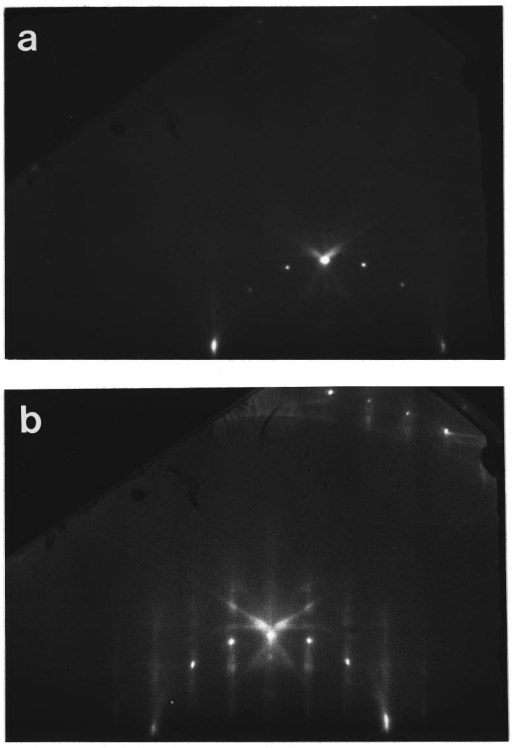

FIG. 3. RHEED patterns ($[11\bar{2}]$ incidence) of the investigated surface at (a) 870 K and (b) RT.

DW's disappear and the perfect $\sqrt{3}$-Au layer covers the whole surface. We can assume that the most probable explanation for the $\alpha\sqrt{3}$-Au$\rightarrow\gamma\sqrt{3}$-Au phase transition is an evaporation of the DW's into a gas of pointlike defects (PD's) proposed recently by Lyuksyutov *et al.*[10] We observed experimentally a transition into a commensurate phase from the apparently incommensurate structure under the condition of constant coverage as a function of increasing temperature; thereby, according to the theoretical study by Lyuksyutov *et al.*,[10] the most important property of the DW evaporation transition is experimentally verified. To our knowledge, this phenomenon was previously reported for the Ba/Mo(110) (Ref. 11) and Te/Mo(110) (Ref. 12) surfaces only and this is an observation of the DW evaporation in the metal/Si(111) system.

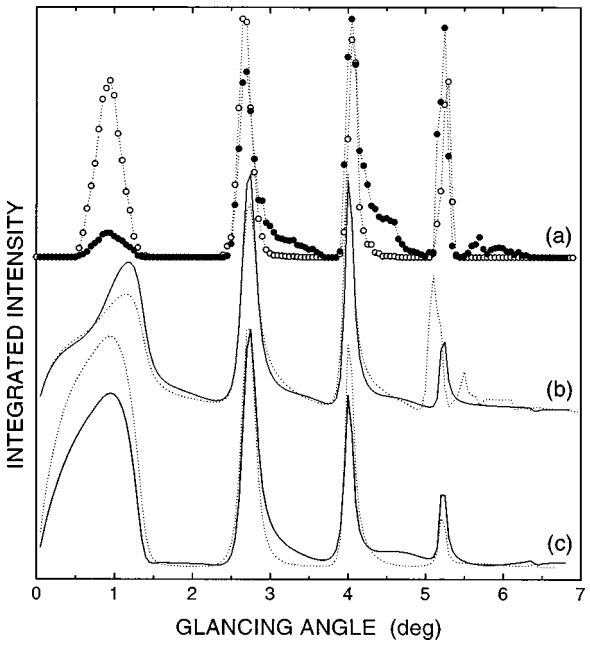

FIG. 4. (a) Experimental rocking curves taken at $[21\bar{3}]$ incidence at RT (filled circles) and 870 K (open circles), (b) the results of the dynamical one-beam (solid line) and five-beam (dotted line) calculations for the CHCT-1 model, and (c) our fitting for $\alpha\sqrt{3}$-Au and $\gamma\sqrt{3}$-Au phases (solid and dotted lines, respectively).

The dynamical one-beam calculation for the $[21\bar{3}]$ azimuth was conducted with the parameters for the interlayer distances and atomic densities of each layer for all proposed structural models[13–17] of the $\sqrt{3}$-Au surface. The results were compared with experimental data. We found that the conjugate honeycomb-chained-trimer (CHCT-1) model proposed by Ding *et al.*[13] is the only one that fits the experimental RC for the $\alpha\sqrt{3}$-Au surface, but any one of these calculated RC's bear no resemblance to the experimental one for the $\gamma\sqrt{3}$-Au phase.

The calculated RC for the CHCT-1 model is shown in Fig. 4(b) by a solid line; a dotted line shows the result of the five-beam dynamical calculation. Our calculation revealed that the most sensitive parameter is the Au-Si interlayer distance (0.56 Å), which was obtained by the total-energy calculation[13] and proved later by full-dynamical low-energy electron diffraction (LEED) intensity analysis.[18] Any deviation of the Au-Si interlayer distance from the value of 0.56 ($\pm$0.015) Å caused dramatic changes in the calculated RC's, which could not be corrected by modification of the other parameters. The same result was reported by Quinn *et al.*[18] for full-dynamical LEED intensity analysis. The features of the CHCT-1 model such as the missing top silicon layer and 1-ML Au coverage were found to be also very significant for the one-beam dynamically calculation.

As one can see from the comparison of the calculated RC for the CHCT-1 model with the experimental one, there is not full agreement between theory and experiment, which was also the case for the LEED intensity analysis.[18] For the calculated RC the positions of the 2.75°, 4°, and 5.25° peaks and their shoulders fit the experimental data satisfactorily,

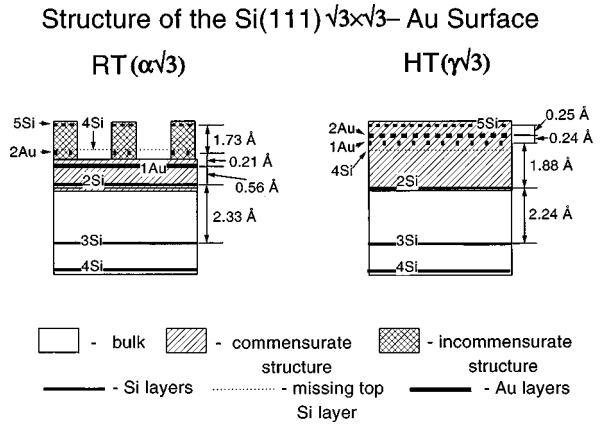

FIG. 5. Distribution of the atomic densities in the surface parallel layers for the (a) $\alpha\sqrt{3}$-Au and (b) $\gamma\sqrt{3}$-Au phases. Error bars for the positions of the surface parallel layers are shown in Tables I and II.

TABLE I. Distribution of the atomic densities in the surface parallel layers of the Si(111)$\alpha(\sqrt{3}\times\sqrt{3})R30°$-Au structure (RT). All layers are schematically shown in Fig. 4(a).

Layer N	Distance from the bulklike surface (4Si layer)	Layer density [in Si(111) atomic density units]	Description
1Si	bulklike $\pm$ 0.01 Å	1	bulk
2Si	bulklike $\pm$ 0.01 Å	1	substrate
3Si	-0.80 ± 0.015 Å	1	commensurate
1Au	-0.24 ± 0.015 Å	1	overlayer
4Si	0.00 Å	0	missing
2Au	-0.03 ± 0.015 Å	0.25 ± 0.03	domain
5Si	1.7 ± 0.1 Å	0.67 ± 0.03	walls

but the position of the peak at about 1° is very different. The latter peak is very sensitive to the atomic structure of the surface and the coincidence of the calculated and experimental RC's in this angle region is an important criterion for the validity of the model. For the further fitting of the calculated RC to the experimental data we speculated that the additional atomic density, which can be associated with domain walls, exists on the top of the ordered $\sqrt{3}$-Au structure.

Our best fitting is shown by the solid line in Fig. 4(c) and the corresponding surface structure is presented in Fig. 5(a) and Table I. We have found that the calculated RC for the CHCT-1 model can be corrected and completely fitted to the experimental data by introducing an additional atomic density of Si ($\Theta_{\mathrm{Si}}^{\mathrm{DW}}=0.67\pm0.03$ ML) and Au ($\Theta_{\mathrm{Au}}^{\mathrm{DW}}=0.25\pm0.03$ ML) atoms on top of the ordered $\sqrt{3}$-Au surface.

As mentioned above, the calculated RC was very sensitive to the Au coverage in the $\sqrt{3}$-Au structure ($\Theta_{\mathrm{Au}}^{\mathrm{st}}$): Fitting was impossible if $\Theta_{\mathrm{Au}}^{\mathrm{st}}$ was less than 1 ML. We believe that a total Au coverage ($\Theta_{\mathrm{Au}}=\Theta_{\mathrm{Au}}^{\mathrm{st}}+\Theta_{\mathrm{Au}}^{\mathrm{DW}}$) of 1.25 ML is a reasonable value. As shown in Fig. 2, we stopped Au deposition at 24 min, i.e., 4 min after the disappearance of 5×2 diffraction spots or when the whole surface was covered with the $\sqrt{3}$-Au structure. Assuming that after 20 min of Au deposition $\Theta_{\mathrm{Au}}=\Theta_{\mathrm{Au}}^{\mathrm{st}}=1$ ML, we can easily obtain 1.2-ML Au coverage for the investigated surface, which gives us excellent agreement with the calculated value.

It should be particularly emphasized that according to our data, domain walls for this particular surface consist approximately 1/3 of Au and 2/3 of Si atoms, which can be an explanation of a high concentration of the domain walls on the $\sqrt{3}$-Au regions even though the $\sqrt{3}$ and 5×2 structures coexist.[2]

Different from the $\alpha\sqrt{3}$-Au structure, none of the RC's calculated for any models proposed previously for the $\sqrt{3}$-Au structure resembles experimental data for the γ phase. Our best fitting for this case is shown by the dotted line in Fig. 4(c) and the corresponding surface structure is presented in Fig. 5(b) and Table II. As clearly seen from the comparison of Tables I and II, the interlayer distances and the atomic densities of all layers involved in the surface phase formation are different for both surfaces. However, in spite of how the atomic densities of the 3Si($\Theta_{3\mathrm{Si}}$), 1Au($\Theta_{1\mathrm{Au}}$), 2Au($\Theta_{2\mathrm{Au}}$), and 5Si($\Theta_{5\mathrm{Si}}$) layers are considerably different for RT and HT phases, the values of $\Theta_{3\mathrm{Si}}+\Theta_{5\mathrm{Si}}$ and $\Theta_{1\mathrm{Au}}+\Theta_{2\mathrm{Au}}$ are the same for both phases within an accuracy of ±0.05 ML. The atomic densities in Table II present the *best* fitting for the HT $\sqrt{3}$-Au structure, but, according to our results, the redistribution of Au atoms between 1Au and 2Au layers within ±0.125 ML and Si atoms between 3Si and 5Si layers within ±0.178 ML does not change essentially the calculated RC's. This is the reason why we denoted the 3Si layer as a part of the surface phase, but not part of the relaxed substrate.

As is well known from the STM images,[2–4] DW's exist always on the $\sqrt{3}$-Au surface at RT and the origination of the additional atomic density is apparent for this case. For the $\gamma\sqrt{3}$-Au structure the description of each atomic layer is not so evident. We assume that when T_s increases the distance between the Au and Si layers ($z_{\mathrm{Au\text{-}Si}}$) in the commensurate structure increases and reaches eventually 2.12 ± 0.08 Å (see Table II) at $T_s\approx850$ K. Both of these layers contain vacancies: Each eighth atom is missing in the Au layer (2Au) and

TABLE II. Distribution of the atomic densities in the surface parallel layers of the Si(111)$\gamma(\sqrt{3}\times\sqrt{3})R30°$-Au structure (870 K). All layers are schematically shown in Fig. 4(b).

Layer N	Distance from the bulklike surface (4Si layer)	Layer density [in Si(111) atomic density units]	Description
1Si	bulklike $\pm$ 0.005 Å	1	bulk
2Si	bulklike $\pm$ 0.005 Å	1	substrate
3Si	-0.90 ± 0.015 Å	0.833 ± 0.178	commensurate
2Au	1.22 ± 0.06 Å	0.875 ± 0.125	structure
1Au	0.98 ± 0.06 Å	0.375 ± 0.125	composite
5Si	1.47 ± 0.025 Å	0.833 ± 0.178	PD's

each sixth atom is missing in the Si layer (3Si). The position of the additional atom density changes too: Additional Au atoms (1Au) are located between 2Au and 3Si layers and additional Si atoms remain on top of the surface. Our recent studies indicate that atoms incorporated into the 2Au and 3Si layers form composite PD's[19] whose concentration is about 0.12 ML for these surface conditions. To prove this speculation the exact many-beam dynamical calculation must be conducted.

CONCLUSIONS

In summary, we have observed experimentally the transformation from an incommensurate structure with DW's ($\alpha\sqrt{3}$-Au) to a commensurate phase with PD's ($\gamma\sqrt{3}$-Au), namely, vacancies and interstitials, under the condition of constant coverage as a function of increasing temperature, which is an experimental verification of the DW evaporation transition. To our knowledge, this is the first observation of the DW evaporation in the metal/Si(111) system. We have determined the structure perpendicular to the surface of the $\alpha\sqrt{3}$-Au and $\gamma\sqrt{3}$-Au phases using one-beam RHEED dynamical calculations. Our experimental data and calculation results show that the additional atomic density exists on both surfaces: These atoms are assumed to be incorporated into DW's on the $\alpha\sqrt{3}$-Au phase and to form PD's in the $\gamma\sqrt{3}$-Au structure.

ACKNOWLEDGMENTS

It is our pleasure to acknowledge discussions with Professor I.F. Lyuksyutov and the critical reading and kind advice on the manuscript by Professor M.W. Corr. This work was carried out under financial support from The Ministry of Education, Science, Sports and Culture [Grant-in-Aid for Creative Basic Research (No. 09NP1201) and Grant-in-Aid (No. 96092)]. E.A.K. acknowledges the Japan Society for the Promotion of Science for financial support. All calculations were performed at the Computation Center of Nagoya University.

[1] H. R. Bishop and J. C. Riviere, Br. J. Appl. Phys., J. Phys. D **2**, 1635 (1969).
[2] J. Nogami, A. A. Baski, and C. F. Quate, Phys. Rev. Lett. **65**, 1611 (1990).
[3] J. Nogami, A. A. Baski, and C. F. Quate, Phys. Rev. Lett. **65**, 2211 (1990).
[4] T. Nagao, K. Tshuchie, C. Vogles, H. Pfnür, and S. Hasegawa (unpublished).
[5] K. Higashiyama, S. Kono, and T. Sagawa, Jpn. J. Appl. Phys., Part 2 **25**, L117 (1986).
[6] A. Ichimiya, Jpn. J. Appl. Phys., Part 1 **22**, 176 (1983).
[7] A. Ichimiya, Surf. Sci. Lett. **192**, L893 (1987).
[8] Y. Horio and A. Ichimiya, Surf. Sci. **133**, 393 (1983).
[9] S. Kohmoto and A. Ichimiya, Surf. Sci. **223**, 400 (1989).
[10] I. F. Lyuksyutov, H. Pfnür, and H.-U. Everts, Europhys. Lett. **33**, 673 (1996).
[11] E. V. Klimenko, E. M Litvinova, I. F. Lyuksyutov, A. G. Naumovets, and I. N. Zasimovich, Surf. Sci. **271**, 244 (1992).
[12] M. Stolzenberg, I. F. Lyuksyutov, and E. Bauer, Phys. Rev. B **48**, 2675 (1993).
[13] Y. G. Ding, C. T. Chan, and K. M. Ho, Surf. Sci. Lett. **275**, L691 (1992).
[14] K. Oura, M. Katayama, F. Shoji, and T. Hanawa, Phys. Rev. Lett. **55**, 1486 (1985).
[15] J. H. Huang and R. S. Williams, Phys. Rev. B **38**, 4022 (1988).
[16] M. Chester and T. Gustafsson, Surf. Sci. **256**, 135 (1991).
[17] Y. Kuwahara, S. Nakatani, M. Takahashi, M. Aono, and T. Takahashi, Surf. Sci. **310**, 226 (1994).
[18] J. Quinn, F. Jona, and P. M. Marcus, Phys. Rev. B **46**, 7288 (1992).
[19] E. A. Khramtsova, H. Sakai, K. Hayashi, and A. Ichimiya (unpublished).